Mössbauer spectra of **1** (X = RCOO, Y = PPh_2) consist of a single quadrupole doublet indicating equivalence of the two iron sites. Quadrupole splittings (1.55–1.76 mm s^{-1}) are larger than values (≤1.0 mm s^{-1}) associated with distorted octahedral stereochemistry,[12] and there is a marked increase in Δ on replacement of a one-carbon, three-electron bridge in **2** (R = H, R′ = C_6H_{11}-c) (Δ = 0.65 mm s^{-1}) by a carboxylate. We attribute this to a lengthening of the Fe–Fe bond and an increase in planarity of the $Fe_2(X)(Y)$ ring system together with a greater charge imbalance in the iron bonding orbitals generated by the presence of two cis bridging ligands (PPh_2 and RCOO) of very different electronic characteristics. Isomer shifts for **1** (X = RCOO, Y = PPh_2) are shifted toward the values for covalent Fe(II) compounds, i.e., more positive compared to those of their precursors **2**.

We have recently suggested[4] that ^{31}P NMR chemical shifts for phosphido bridges in binuclear iron carbonyls of type **1**, where the second bridging ligand X is a one-carbon, three-electron or a two-carbon, three-electron donor, are sensitive to the nature of X. Thus for example complexes of type **2** have δ(^{31}P; PPh_2) in the range of 140–160 downfield of 85% H_3PO_4 whereas in **5** where two carbon atoms are involved in bridging, δ(^{31}P; PPh_2) values lie between 180 and 190. From the wealth of X-ray data available for these derivatives[4-6,13] it is apparent that high δ values are associated with longer Fe–Fe bond lengths and larger valence angles at the bridging atom.[14] This correlation even extends to $Fe_2(CO)_6\{CH_2C(Ph)NMe\}(PPh_2)$ (**6**) (δ(^{31}P) = 198.5, Fe(1)–Fe(2) = 2.704 (1) Å, Fe(1)–P–Fe(2) = 75.6 (0)°) where an $FeCH_2C(Ph)N(Me)Fe$ ring is present.[15] For the carboxylates **1**, ^{31}P shifts lie close to the value for **6** but well above the values for the halides which are much closer to the range found for type **2** compounds.[16] The structural similarity between the five-membered $FeOC(R)OFe$ and $FeCH_2C(Ph)N(Me)Fe$ rings in **1** and **6**, respectively, is striking. On the basis of an empirical correlation of δ(^{31}P) vs. Fe–P–Fe for complexes of types **1**, **2**, **5**, and **6** we predict a bond angle of ~73° for the carboxylates **1** with an associated Fe–Fe bond length of 2.68 Å. For **1** (X = I) an Fe–P–Fe angle of ~70° is predicted.[17] We are currently measuring shifts for phosphido bridges in a range of binuclear iron complexes with and without metal–metal bonds in an attempt to determine whether δ(^{31}P) M–P–M bond angle correlations are structurally valid for a wider variety of complexes.

Finally we note that the facile reactions of the dipolar organometallic complexes **2** with protic acids demonstrate the not unexpected susceptibility of these molecules to electrophilic attack. In principle, electrophilic attack could occur either at the formally negative bridging carbon atom or, alternatively, on the iron–iron bond. Mechanistic studies designed to establish the intital site of attack are in progress.

Acknowledgment. We thank the National Science and Engineering Research Council of Canada for financial support.

Registry No. **1** (X = Cl, Y = PPh_2), 71000-92-5; **1** (X = B, Y = PPh_2), 71000-93-6; **1** (X = I, Y = PPh_2), 71000-94-7; **1** (X = HCOO, Y = PPh_2), 71000-95-8; **1** (X = CH_3COO, Y = PPh_2), 71031-56-6; **1** (X = C_2H_5COO, Y = PPh_2), 71000-96-9; **1** (X = CF_3COO, Y = PPh_2), 71031-57-7; **2** (R = H, R′ = CH_3), 70657-55-5; **2** (R = H, R′ = C_2H_5), 70657-57-7; $Fe_2(CO)_6(C_2Ph)(PPh_2)$, 52970-25-9; $MeNH_2$, 74-89-5; $EtNH_2$, 75-04-7.

References and Notes

(1) E. Koerner von Gustorf, J. C. Hogan, and R. Wagner, *Z. Naturforsch.*, **276**, 140 (1972).
(2) M. Kilner and C. Midcalf, *Chem. Commun.*, 944 (1971).
(3) F.-W. Grevels, D. Schulz, E. Koerner von Gustorf, and D. St. P. Bunbury, *J. Organomet. Chem.*, **91**, 341 (1975).
(4) A. J. Carty, G. N. Mott, N. J. Taylor, and J. E. Yule, *J. Am. Chem. Soc.*, **100**, 3051 (1978).
(5) A. J. Carty, N. J. Taylor, H. N. Paik, W. Smith, and J. E. Yule, *J. Chem. Soc., Chem. Commun.*, 41 (1976).
(6) (a) H. A. Patel, R. G. Fischer, A. J. Carty, D. V. Naik, and G. J. Palenik, *J. Organomet. Chem.*, **60**, C49 (1973); (b) W. F. Smith, J. Yule, N. J. Taylor, H. N. Paik, and A. J. Carty, *Inorg. Chem.*, **16**, 1593 (1977).
(7) P. M. Treichel, W. K. Dean, and J. C. Calabrese, *Inorg. Chem.*, **12**, 2908 (1973).
(8) G. Bor, *J. Organomet. Chem.*, **94**, 181 (1975).
(9) The frequency separations ($\nu_{as}(CO_2) - \nu_s(CO_2)$) for **1** (X = RCOO) themselves do not exclusively prove symmetrical bridging since instances are known where small Δν values occur for monodentate carboxylates. An example is $Ni(H_2O)_4(CH_3COO)_2$ which has $\Delta\nu = 107$ cm^{-1} and where $\nu_{as}(CO_2)$ is strongly affected by hydrogen bonding. See: (a) T. C. Downie, W. Harrison, E. S. Raper, and M. A. Hepworth, *Acta Crystallogr., Sect. B*, **27**, 706 (1971); (b) K. Nakamoto, J. Fujita, S. Tanaka, and M. Kobayashi, *J. Am. Chem. Soc.*, **79**, 4904 (1957).
(10) The $\nu(CO_2)$ frequencies in **1** (X = RCOO, Y = PPh_2) can be compared with values in $Cr_2(CH_3COO)_4$ ($\Delta\nu_{CO_2} = 149$ cm^{-1}) (G. Costa, E. Pauluzzi, and A. Puxeddu, *Gazz. Chim. Ital.*, **87**, 885 (1957)) and $Rh_2(CH_3COO)_4$ ($\Delta\nu_{CO_2} = 155$ cm^{-1}) (S. A. Johnson, H. R. Hunt, and H. M. Neumann, *Inorg. Chem.*, **2**, 960 (1963)) which contain symmetrical bidentate carboxylates
(11) Examples of unsymmetrical bridging of carboxylates in symmetrical complexes are known. See T. Birchall and J. P. Johnson, *Can. J. Chem.*, **57**, 160 (1979), and references therein.
(12) N. N. Greenwood and T. C. Gibb, "Mossbauer Spectroscopy", Chapman and Hall, London, 1971, pp 221–3.
(13) A. J. Carty, G. N. Mott, N. J. Taylor, G. Ferguson, M. A. Khan, and P. J. Roberts, *J. Organomet. Chem.*, **149**, 345 (1978).
(14) For example in $Fe_2(CO)_6\{CHC(Ph)NHC_6H_{11}\text{-}c\}(PPh_2)$,[4] δ($^{31}P$) = 158.3, Fe(1)–Fe(2) = 2.576 (1) Å, and Fe(1)–P–Fe(2) = 70.5 (0)°, whereas for $Fe_2(CO)_6\{C(NHC_6H_{11}\text{-}c)CH(Ph)\}PPh_2$,[4] δ($^{31}P$) = 187.9, Fe(1)–Fe(2) = 2.628 (1) Å, and Fe(1)–P–Fe(2) = 72.4 (0)°.
(15) A. J. Carty, G. N. Mott, and N. J. Taylor, unpublished results.
(16) A referee has pointed out that there are some similarities in the trends of ^{31}P chemical shifts for complexes of type **1** (Y = PPh_2, X = Cl, Br, I, RCOO) and **6** with ^{31}P shifts in phosphorus chelate complexes. Thus in compounds where the phosphido bridge is part of a six-membered ring (e.g., **1**, Y = PPh_2, X = RCOO; and **6**) shifts are 30–40 ppm downfield of values in the halide-bridged complexes where the phosphorus atom is part of a four-membered ring. For analogous chelate rings differences of 15–30 ppm are apparent. See P. E. Garrou, *Inorg. Chem.*, **14**, 1435 (1975).
(17) The chloride complex $Fe_2(CO)_6(Cl)(PPh_2)$ crystallizes on long standing. A single-crystal X-ray analysis has confirmed the molecular structure **1** (X = Cl, Y = PPh_2) with an Fe–Fe bond length of 2.560 (1) Å and an Fe–P–Fe bond angle of 69.7 (0)°.

Contribution from the Chemistry Department, University of California, Berkeley, California 94720

Dialkylbis[bis(trimethylsilyl)amido]zirconium(IV) and -hafnium(IV). Preparation and Reaction with Carbon Dioxide and *tert*-Butyl Isocyanide

Richard A. Andersen

Received March 29, 1979

Dichlorobis[bis(trimethylsilyl)amido]zirconium(IV) and -hafnium(IV) have been prepared from the metal tetrachloride (M = Zr or Hf) and lithium bis(trimethylsilyl)amide in diethyl ether. A chloride ligand in each compound can be replaced with a tetrahydroborate group, yielding $(Cl)(BH_4)M[N(SiMe_3)_2]_2$, M = Zr or Hf. The dimethyl derivatives, $Me_2M[N(SiMe_3)_2]_2$, where M is Zr or Hf, can be prepared from the dichloro derivatives and dimethylmagnesium. Bis[(trimethylsilyl)methyl]- and diethylhafnium derivatives were similarly prepared. The hafnium dialkyls react with carbon dioxide (5–10 atm) at room temperature, yielding the carbamato derivatives $R_2Hf[O_2CN(SiMe_3)_2]_2$, where R = Me, Et, or Me_3SiCH_2. Reaction of the hafnium dialkyls (R = Me or Et) with *tert*-butyl isocyanide takes a different course, yielding $[t\text{-}BuN{=}C(R)]_2Hf[N(SiMe_3)_2]_2$, where R = Me or Et, by way of insertion into the hafnium–carbon bond. The electrophile, CO_2, inserts into the metal–nitrogen bond whereas the nucleophile, *t*-BuNC, inserts into the metal–carbon bond.

0020-1669/79/1318-2928$01.00/0

Table I. Analytical and Physical Properties of $[(Me_3Si)_2N]_2MX_2$

compd	mp, °C	anal., % calcd C	H	N	other	found C	H	N	other	IR, cm^{-1} M-N	other
$[(Me_3Si)_2N]_2ZrCl_2$	53-53	29.9	7.47	5.81	14.7[a]	29.7	7.72	5.77	14.2[a]	420	388[b]
$[(Me_3Si)_2N]_2HfCl_2$	44-45	25.3	6.32	4.92	12.5[a]	25.4	6.29	4.86	12.1[a]	418	405[b]
$[(Me_3Si)_2N]_2ZrMe_2$	ca. 20	38.1	9.52	6.35		37.8	9.51	6.30		370	
$[(Me_3Si)_2N]_2HfMe_2$	ca. 20	31.8	7.95	5.30		31.0	7.91	5.23		370	
$[(Me_3Si)_2N]_2HfEt_2$	65-67	34.5	8.27	5.03		35.0	8.21	5.00		380	
$[(Me_3Si)_2N]_2Hf(CH_2SiMe_3)_2$	91-92	35.7	8.62	4.16		35.1	8.57	4.08		395	
$[(Me_3Si)_2N]_2Zr(Cl)(BH_4)$	42-44	31.2	8.67	6.07	7.69[a]	31.0	8.58	6.01	7.53[a]	415	355[b]
$[(Me_3Si)_2N]_2Hf(Cl)(BH_4)$	55-57	26.2	7.29	5.10	6.47[a]	25.8	7.19	5.03	6.39[a]	not measd	
$[(Me_3Si)_2NCO_2]_2HfMe_2$	81-83	31.1	6.81	4.54		31.0	6.75	4.45			1575[c]
$[(Me_3Si)_2N]_2Hf[C(Me)=N\text{-}t\text{-}Bu]_2$	166-168	41.5	8.64	8.06		40.9	8.58	8.00		388	1565[d]
$[(Me_3Si)_2NCO_2]_2HfEt_2$	58-60	33.5	7.14	4.34		32.9	7.03	4.28			1555[c]
$[(Me_3Si)_2N]_2Hf[C(Et)=N\text{-}t\text{-}Bu]_2$	ca. 20	42.7	8.81	7.69		43.2	8.86	7.75		390	1565[d]
$[(Me_3Si)_2NCO_2]_2Hf(CH_2SiMe_3)_2$	ca. 20	34.7	7.63	3.68		34.1	7.59	3.59			1550[c]

[a] Chloride. [b] M-Cl. [c] $\nu_{asy}(CO_2)$. [d] $\nu(C{=}N)$.

Table II. Spectroscopic Properties of $[(Me_3Si)_2N]_2MX_2$

compd	^{1}H NMR[a,b] $(Me_3Si)_2N$	Me or Me_3Si	CH_2	other	^{13}C{^{1}H} NMR[c] $(Me_3Si)_2N$	Me or Me_3Si	CH_2	other
$[(Me_3Si)_2N]_2ZrCl_2$	0.57 s				4.46			
$[(Me_3Si)_2N]_2HfCl_2$	0.62 s				4.79			
$[(Me_3Si)_2N]_2ZrMe_2$	0.44 s	0.94 s			4.90	48.8		
$[(Me_3Si)_2N]_2HfMe_2$	0.45 s	0.75 s			4.95	60.2		
$[(Me_3Si)_2N]_2HfEt_2$	0.49 s	1.89 (t, J = 7 Hz)	1.05 (q, J = 7 Hz)		5.16	14.1	74.6	
$[(Me_3Si)_2N]_2Hf(CH_2SiMe_3)_2$	0.67 s	0.54 s	0.67 s		5.91	3.40	76.3	
$[(Me_3Si)_2N]_2Zr(Cl)(BH_4)$	0.50 s			2.57 (q, J_{BH} = 85 Hz)				
$[(Me_3Si)_2N]_2Hf(Cl)(BH_4)$	0.54 s			3.11 (q, J_{BH} = 85 Hz)				
$[(Me_3Si)_2NCO_2]_2HfMe_2$	0.48 s	1.20			5.00	60.2		183[d]
$[(Me_3Si)_2N]_2Hf[C(Me)=N\text{-}t\text{-}Bu]_2$	0.45 s	2.77 s		1.34 s[e]	6.33	29.7		30.2[e,f]
$[(Me_3Si)_2NCO_2]HfEt_2$	0.46 s	1.96 t, J = 8 Hz)	1.11 (q, J = 8 Hz)		6.73	14.0	74.5	182[d]
$[(Me_3Si)_2N]_2Hf[C(Et)=N\text{-}t\text{-}Bu]_2$	0.50 s	1.44 (t, J = 7 Hz)	3.17 (q, J = 7 Hz)	1.46 s[e]	7.28	11.9	29.6	30.9[e] 32.2[g] 262[h]
$[(Me_3Si)_2NCO_2]_2Hf(CH_2SiMe_3)_2$	0.45 s	0.39 s	0.63 s		5.99	3.48	76.3	185[d]

[a] δ relative to Me_4Si = 0; positive value is to high frequency, in benzene. [b] s = singlet, t = triplet, q = quartet. [c] Same as *a* except in benzene-d_6. [d] $(Me_3Si)_2NCO_2$. [e] N-*t*-CMe_3. [f] The quaternary carbon atoms were not observed. [g] N-*t*-CMe_3. [h] HfC(Et)=N.

Metal–bis(trimethylsilyl)amido derivatives, $[(Me_3Si)_2N]_xM$, of the second- and third-row transition series are exceedingly rare. This is to be contrasted with the large number of these types of compounds known for the first-row transition series.[1-3] The tris(silylamido) derivatives of the type $[(Me_3Si)_2N]_3MX$, where M is zirconium or hafnium and X is chloro or methyl, have recently been described.[4] Some gold(I) phosphine or arsine complexes, $[(Me_3Si)_2N]AuL$, are also known.[5]

The chlorotris[bis(trimethylsilyl)amido]metal compounds of zirconium or hafnium are readily prepared from either 2 or 3 molar equiv of sodium bis(trimethylsilyl)amide and the metal tetrachloride in diethyl ether.[4] In contrast, addition of 2 molar equiv of lithium bis(trimethylsilyl)amide to either zirconium or hafnium tetrachloride in diethyl ether yields the disubstituted derivatives $[(Me_3Si)_2N]_2MCl_2$, where M is zirconium or hafnium. Analytical data and some physical properties are shown in Table I, and spectroscopic properties are in Table II. The bis derivatives, $[(Me_3Si)_2N]_2MCl_2$, are rather more air and moisture sensitive than the tris derivatives, $[(Me_3Si)_2N]_3MCl$, which are air stable. Further, the disubstituted compounds rapidly yield a precipitate of silver chloride upon contact with an acidic solution of silver nitrate.

A chloride ligand can be replaced by a tetrahydroborate group, yielding $(Cl)(BH_4)M[N(SiMe_3)_2]_2$ where M is Zr or Hf with lithium tetrahydroborate in diethyl ether. Use of excess lithium tetrahydroborate does not result in further substitution. The infrared spectra of these mono(tetrahydroborate) derivatives show that the BH_4 group is bonded in a tridentate fashion. The zirconium compound has a single absorption at 2530 cm^{-1} due to terminal B–H groups and two absorptions in the B–H–M stretching frequency region at 2200 and 2140 cm^{-1}. The infrared spectrum of the hafnium analogue is similar, showing absorptions at 2545, 2220, and 2155 cm^{-1}. This absorption pattern is indicative of the tetrahydroborate group being tridentate.[6,7] The tetrahydroborate group in both six-coordinate compounds is fluxional on the NMR time scale since only a 1:1:1:1 quartet is observed (180 MHz) at δ 3.11 (J_{BH} = 85 Hz) for the hafnium compound at room temperature or at −80 °C. The zirconium compound is similar, the quartet being centered at δ 2.57 (J_{BH} = 84 Hz).

The dichloro compounds yield the dimethyl derivatives $Me_2M[N(SiMe_3)_2]_2$ upon reaction with dimethylmagnesium in diethyl ether. The dialkyls are colorless liquids at room temperature which may be crystallized from pentane at low temperature. They are volatile enough to afford monomeric ions in the mass spectrometer. The bis[(trimethylsilyl)methyl]hafnium derivative can be prepared similarly.

Dimethylbis[bis(trimethylsilyl)amido]hafnium takes up 2 equiv of carbon dioxide (5 atm) in pentane at room temperature, affording "$Me_2Hf[N(SiMe_3)_2]_2(CO_2)_2$". The carbon

dioxide product could be either an acetate (I), from insertion

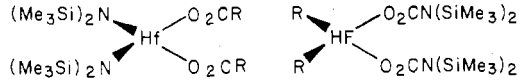

I II

into the hafnium–carbon bond, or a carbamate (II), from insertion into the hafnium–nitrogen bond. The infrared spectrum has an absorption at 1575 cm^{-1} due to the asymmetric CO_2 stretching frequency which is consistent with either isomer. The ^1H NMR spectrum is of no diagnostic value since the methyl–hafnium resonance is only slightly deshielded, and the Me_3Si resonance is essentially the same as that found in the parent compound. The $^{13}C\{^1H\}$ NMR spectrum however clearly shows that the insertion has occurred at the amide nitrogen atom since the resonance due to the methyl–hafnium carbon atom δ 60.2 is essentially identical with that found in the starting dialkyl. The methyl carbon atom resonance of an acetate is generally in the range δ 20–35.[8] Thus, the carbamate formulation (II, R = Me) is implicated. In order to test this further we allowed $(Me_3SiCH_2)_2Hf[N(SiMe_3)_2]_2$ to react with carbon dioxide (10 atm). The product, $(Me_3SiCH_2)_2Hf[N(SiMe_3)_2]_2(CO_2)_2$, has ^1H and $^{13}C\{^1H\}$ NMR spectra essentially identical with those of the parent dialkyl though the latter spectrum contains a resonance at δ 185 due to the carboxy carbon atom. This further strengthens our contention that carbon dioxide has inserted into the hafnium–nitrogen bond.

Use of a dialkyl derivative which yields a more complex and informative ^1H NMR spectrum would be desirable; the diethyl derivative would be ideal. Unfortunately, transition-metal ethyl derivatives are not common since the β-hydrogen elimination process is a very favorable one.[9] We have, however, been able to prepare $Et_2Hf[N(SiMe_3)_2]_2$ as a white, crystalline solid which melts at 65 °C without decomposition. The reason for this thermal stability is probably a steric one. The voluminous (trimethylsilyl)amido ligands increase the steric hindrance about the metal atom preventing a β-hydrogen atom of an ethyl group from approaching the hafnium atom at a distance close enough to react. Consequently, the generally low activation energy β-hydrogen elimination process is blocked, and $Et_2Hf[N(SiMe_3)_2]_2$ is thermally stable.

The diethyl derivative reacts with carbon dioxide (10 atm) at room temperature, affording the bis[(trimethylsilyl)carbamato] derivative (II, R = Et). This is readily shown by the proton nuclear magnetic resonance spectrum (Table II), the principal features being the high-field quartet at δ 1.11 and the low-field triplet at δ 1.96, due to the methylene and methyl resonances, respectively. Further, the similarity of the $^{13}C\{^1H\}$ NMR spectrum to that of the parent dialkyl indicates beyond reasonable doubt that carbon dioxide inserts into the metal–nitrogen bond of $R_2Hf[N(SiMe_3)_2]_2$, yielding the carbamato derivatives.

The infrared spectra of the three carbamates show absorptions at ca. 1580 cm^{-1} due to the asymmetric CO_2 stretching frequency. This low-frequency absorption is most likely due to bidentate coordination. Since neither the free acid, $(Me_3Si)_2NCO_2H$, nor complexes of the $(Me_3Si)_2NCO_2$ group have been described, we have no compounds available for comparison. However, if the analogy of a carbamate group with an acetate group is valid, then we can say that the carbamate ligand is bidentate since bidentate acetates absorb in the infrared at ca. 1500–1600 cm^{-1}, whereas monodentate acetates absorb at ca. 1700 cm^{-1}.[10] Caution, however, must be exercised since bidentate dialkylcarbamate absorptions have been observed as high as 1682 cm^{-1}.[11] Since there is neither a steric nor an electronic reason to favor monodentate coordination, we prefer the bidentate one. If this is accepted we have a further stereochemical problem to deal with, viz., trans or cis isomers, III or IV, respectively. If the cis isomer

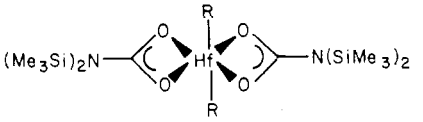

III

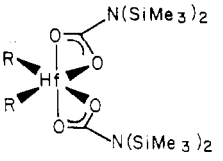

IV

(IV) is correct, the methylene protons are diastereotopic and will give rise to an AB spectrum. If isomer III is correct, then the methylene protons are equivalent, and a single resonance will be observed in the proton NMR spectrum. Unfortunately, the observation of a single methylene resonance (Table II) does not prove anything since the molecule could be fluxional.

The mechanism of carbon dioxide insertion might be viewed as a simple nucleophilic substitution by the amide nitrogen atom on the electron-poor carbonyl carbon atom. However, it has recently been shown that the presence of free amine in solutions of dialkylamido–metal complexes catalyzes CO_2 insertion.[11] Consequently, further speculation on the mechanism is unwarranted.

Dimethylbis[bis(trimethylsilyl)amido]hafnium, though not the bis[(trimethylsilyl)methyl] analogue, reacts with *tert*-butyl isocyanide at room temperature, yielding a 2:1 complex, $Me_2Hf[N(SiMe_3)_2]_2(t\text{-BuNC})_2$. The complex is not a simple coordination complex since the infrared spectrum has ν(CN) at 1565 cm^{-1}, in the region of a carbon–nitrogen double bond rather than a triple bond.[12] The proton and carbon NMR spectra show a singlet for the methyl–hafnium resonance at δ 2.77 and 29.7, deshielded and shielded, respectively, relative to those in the parent complex. This behavior is expected when a methyl group is bonded to a carbon atom rather than to an electropositive metal atom. The complex is then formulated as an insertion into a hafnium–carbon bond rather than into a hafnium–nitrogen bond, $[(Me_3Si)_2N]_2Hf[C(Me)=N\text{-}t\text{-Bu}]_2$.

The diethyl derivative, $Et_2Hf[N(SiMe_3)_2]_2$, behaves similarly, affording $[t\text{-BuN}=CEt]_2Hf[N(SiMe_3)_2]_2$. The proton NMR is clearly diagnostic for insertion into the hafnium–carbon bond since the methylene and methyl resonances in the complex are deshielded and shielded, respectively, relative to those in $Et_2Hf[N(SiMe_3)_2]_2$. The carbon NMR spectrum is also consistent with this view (Table II).

Again, we must demonstrate whether the complex is uni- or bidentate, V or VI, respectively. A distinction can be made

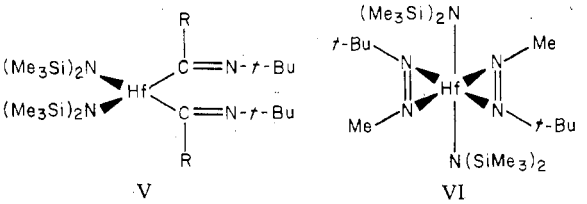

V VI

on the basis of infrared spectroscopy since ν(CN) in $CpMo(CO)_2C(Me)=NPh$ is at 1670 cm^{-1}. The chelate ring has been demonstrated by X-ray crystallography.[13] The chelate ring can be cleaved with $P(OMe)_3$, yielding $CpMo(CO)_2P(OMe)_3[C(Me)=NPh]$ which also has been examined crystallographically.[14] This monodentate complex has ν(CN) at 1570 cm^{-1}. Thus ν(CN) increases upon coordination to a metal center, presumably because the lone pair of electrons on the nitrogen atom is carbon–nitrogen antibonding. The

rather low infrared absorption (1565 cm^{-1}) in the hafnium complex strongly suggests that the coordinated ligand is monodentate (V).[15] The mechanism of this carbon–nitrogen bond reduction can be viewed as shown.

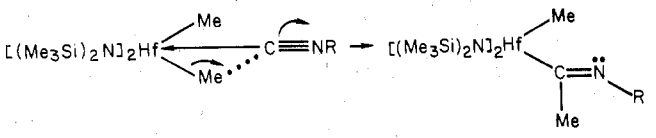

The lack of reaction of the Me_3SiCH_2 analogue with the isocyanide is explained by the inability of the cyanide to form an initial coordination complex since the steric congestion about the metal atom would be too great.

Experimental Section

Analyses were by the microanalytical laboratory of this department. The proton nuclear magnetic resonance spectra were recorded on a Varian T-60. Proton-decoupled carbon nuclear magnetic resonance spectra were recorded on a Nicolet TT-23 machine operating at 25.14 Hz. All operations were performed under nitrogen.

Dichlorobis[bis(trimethylsilyl)amido]zirconium(IV). Lithium bis(trimethylsilyl)amide–0.5-(diethyl ether) complex (6.1 g, 0.031 mol) dissolved in diethyl ether (75 mL) was added to a suspension of zirconium tetrachloride (3.6 g, 0.015 mol) in diethyl ether (50 mL) at 0 °C. After 15 h of stirring, the diethyl ether was evaporated under vacuum, and the residue was extracted into pentane (2 × 50 mL). The solution was filtered, and the filtrate was concentrated to ca. 20 mL and cooled (−70 °C). The white *needles* were collected and dried under vacuum; yield 5.0 g (70%).

Dichlorobis[bis(trimethylsilyl)amido]hafnium(IV). Lithium bis(trimethylsilyl)amide–0.5-(diethyl ether) complex (2.7 g, 0.014 mol) in diethyl ether (30 mL) was added to hafnium tetrachloride (2.2 g, 0.0069 mol) suspended in diethyl ether (50 mL) at room temperature. The suspension was stirred for 36 h. Diethyl ether was removed under vacuum, and the residue was extracted with pentane (50 mL). The pentane extract was filtered, concentrated to ca. 5 mL, and cooled (−70 °C). The white *needles* were collected and dried under vacuum; yield 3.0 g (76%).

Dimethylbis[bis(trimethylsilyl)amido]zirconium(IV). Dimethylmagnesium (4.3 mL of a 0.88 M diethyl ether solution, 0.0038 mol) was added to dichlorobis[bis(trimethylsilyl)amido]zirconium (1.8 g, 0.0038 mol) dissolved in diethyl ether (40 mL) at 0 °C. The suspension was stirred for 8 h at 0 °C. The diethyl ether was evaporated to dryness under vacuum, and the residue was extracted with pentane (40 mL). The extract was filtered, and the filtrate was concentrated to ca. 4 mL and cooled (−70 °C). The colorless *prisms* were isolated and dried under vacuum to give a colorless solid which melts at ca. 20 °C; yield 1.2 g (71%).

Dimethylbis[bis(trimethylsilyl)amido]hafnium(IV). Dimethylmagnesium (3.8 mL of a 0.88 M diethyl ether solution, 0.0033 mol) was added to dichlorobis[bis(trimethylsilyl)amido]hafnium (1.9 g, 0.0033 mol) dissolved in diethyl ether (40 mL) at 0 °C. The suspension was stirred at 0 °C for 8 h. Diethyl ether was removed under vacuum, and the residue was extracted with pentane and then filtered. The filtrate was evaporated to dryness, and the colorless liquid was again dissolved in pentane (20 mL), filtered, and evaporated to dryness, yielding a colorless *liquid* in 87% (1.5 g) yield.

Diethylbis[bis(trimethylsilyl)amido]hafnium(IV). Diethylmagnesium (2.5 mL of a 1.0 M diethyl ether solution, 0.0025 mol) was added to dichlorobis[bis(trimethylsilyl)amido]hafnium (1.4 g, 0.0025 mol) in diethyl ether (35 mL) at 0 °C. The suspension was stirred at 0 °C for 12 h. Diethyl ether was removed under vacuum, and the residue was extracted with pentane (40 mL) and filtered. The filtrate was concentrated to ca. 4 mL and cooled (−70 °C). The colorless *prisms* were collected and dried under vacuum; yield 1.1 g (79%).

Bis[bis(trimethylsilyl)amido]bis[(trimethylsilyl)methyl]hafnium(IV). Bis[(trimethylsilyl)methyl]magnesium (2.5 mL of a 1.0 M diethyl ether solution, 0.0025 mol) was added to a diethyl ether (40 mL) solution of dichlorobis[bis(trimethylsilyl)amido]hafnium (1.4 g, 0.0025 mol) at 0 °C. The suspension was stirred at 0 °C for 6 h. Diethyl ether was evaporated under vacuum, and the residue was extracted with pentane (40 mL) and then filtered. The filtrate was concentrated to ca. 5 mL and then cooled (−70 °C). The colorless *prisms* (1.5 g, 89%) were collected and dried under vacuum.

Chlorobis[bis(trimethylsilyl)amido](tetrahydroborato)zirconium(IV). Lithium tetrahydroborate (0.11 g, 0.0051 mol) in diethyl ether (25 mL) was added to dichlorobis[bis(trimethylsilyl)amido]zirconium (1.2 g, 0.0025 mol) in diethyl ether (30 mL) at 0 °C. The suspension was stirred to 0 °C for 12 h. The diethyl ether was evaporated to dryness, and the residue was extracted with pentane (30 mL). The extract was filtered, and the filtrate was concentrated to ca. 3 mL and cooled (−70 °C). The colorless *needles* were collected and dried under vacuum; yield 1.0 g (88%).

Chlorobis[bis(trimethylsilyl)amido](tetrahydroborato)hafnium(IV). Lithium tetrahydroborate (0.36 g, 0.016 mol) in diethyl ether (30 mL) was added to dichlorobis[bis(trimethylsilyl)amido]hafnium (4.7 g, 0.0082 mol) in diethyl ether (35 mL) at 0 °C. The suspension was stirred for 6 h at 0 °C. The diethyl ether was removed under vacuum, and the residue was extracted with pentane (50 mL). The extract was filtered, and the filtrate was concentrated to ca. 10 mL and cooled (−70 °C). The colorless *prisms* were collected and dried under vacuum; yield 4.1 g (91%).

Reaction of Dimethylbis[bis(trimethylsilyl)amido]hafnium. (a) With Carbon Dioxide. The dialkyl (1.2 g, 0.0023 mol) in pentane (30 mL) was stirred under carbon dioxide (4 atm) at room temperature for 24 h. The volatile material was removed under vacuum, and the white residue was crystallized as colorless *prisms* from pentane (−70 °C) in 70% (1.0 g) yield.

(b) With *tert*-Butyl Isocyanide. *t*-Butyl isocyanide (0.7 mL, an excess) was added to the dialkyl (1.1 g, 0.0021 mol) in toluene (20 mL). After 30 min of stirring, the volatile material was removed under vacuum, and the residue was crystallized from pentane (−70 °C) as colorless *prisms*, yield 67% (1.0 g).

Reaction of Diethylbis[bis(trimethylsilyl)amido]hafnium. (a) With Carbon Dioxide. The dialkyl (0.85 g, 0.0015 mol) in pentane (25 mL) was stirred under carbon dioxide (10 atm) for 12 h at room temperature. The volatile material was removed under vacuum, and the residue was crystallized from pentane (−70 °C) as colorless *prisms* in quantitative yield.

(b) With *tert*-Butyl Isocyanide. *t*-Butyl isocyanide (0.6 mL, an excess) was added to the dialkyl (0.5 g, 0.000 82 mol) in pentane (20 mL), and the solution was stirred for 6 h. The volatile material was removed under vacuum, and the residue was crystallized as colorless *needles* from pentane (−70 °C) in 92% (0.55 g) yield.

Reaction of Bis[bis(trimethylsilyl)amido]bis[(trimethylsilyl)-methyl]hafnium with Carbon Dioxide. The dialkyl (0.75 g, 0.000 99 mol) in pentane (30 mL) was stirred under carbon dioxide (10 atm) for 20 h at room temperature. The volatile material was removed under vacuum, and the residue was crystallized from pentane (−70 °C) as colorless *prisms* which melt at ca. 20 °C. The yield was quantitative.

Acknowledgment. We thank the National Science Foundation for a departmental grant to purchase the nuclear magnetic resonance spectrometer used in this work.

Note Added in Proof. A recent crystal structure analysis of $Cp_2TiC(PH)=N(o\text{-xylyl})$ [van Bolhuis, F.; de Boer, E. J. M.; Teuben, J. H. *J. Organomet. Chem.* **1979**, *170*, 299] shows the iminoacyl ligand to be bidentate and $\nu(CN)$ = 1573 cm^{-1}. Thus, $\nu(CN)$ is not a reliable indicator of denticity.

Registry No. $[(Me_3Si)_2N]_2ZrCl_2$, 70969-28-7; $[(Me_3Si)_2N]_2HfCl_2$, 70969-29-8; $[(Me_3Si)_2N]_2ZrMe_2$, 70969-30-1; $[(Me_3Si)_2N]_2HfMe_2$, 71000-84-5; $[(Me_3Si)_2N]_2HfEt_2$, 70969-31-2; $[(Me_3Si)_2N]_2Hf(CH_2SiMe_3)_2$, 70969-32-3; $[(Me_3Si)_2N]_2Zr(Cl)(BH_4)$, 70982-71-7; $[(Me_3Si)_2N]_2Hf(Cl)(BH_4)$, 70982-72-8; $[(Me_3Si)_2NCO_2]_2HfMe_2$, 70982-73-9; $[(Me_3Si)_2N]_2Hf[C(Me)=N\text{-}t\text{-}Bu]_2$, 70969-33-4; $[(Me_3Si)_2NCO_2]_2HfEt_2$, 70982-69-3; $[(Me_3Si)_2N]_2Hf[C(Et)=N\text{-}t\text{-}Bu]_2$, 70969-34-5; $[(Me_3Si)_2NCO_2]_2Hf(CH_2SiMe_3)_2$, 70982-70-6; $ZrCl_4$, 10026-11-6; $HfCl_4$, 13499-05-3; CO_2, 124-38-9; *tert*-butyl isocyanide, 7188-38-7.

References and Notes

(1) Bürger, H; Wannagat, U. *Monatsh. Chem.* **1963**, *94*, 1007; **1964**, *95*, 1099.
(2) Alyea, E. C.; Bradley, D. C.; Copperthwaithe, R. G. *J. Chem. Soc., Dalton Trans.* **1972**, 1580.
(3) Bradley, D. C.; Chisholm, M. H. *Acc. Chem. Res.* **1976**, *9*, 273.
(4) Andersen, R. A. *Inorg. Chem.* **1979**, *18*, 1724.
(5) Shiotani, A.; Schmidbaur, H. *J. Am. Chem. Soc.* **1970**, *92*, 7003.
(6) Marks, T. J.; Kennelly, W. J.; Kolb, J. R.; Shimp, L. A. *Inorg. Chem.* **1972**, *11*, 2540.

(7) Turner, H. W.; Andersen, R. A.; Zalkin, A.; Templeton, D. H. *Inorg. Chem.* **1979**, *18*, 1221.
(8) Strothers, J. B. "Carbon-13 NMR Spectroscopy"; Academic Press: New York, 1972.
(9) Mowat, W.; Shortland, A.; Yagupsky, G.; Hill, N. J.; Yagupsky, M.; Wilkinson, G. *J. Chem. Soc., Dalton Trans.* **1972**, 533.
(10) Robinson, S. D.; Uttley, M. F. *J. Chem. Soc. Dalton Trans.* **1973**, 1912.
(11) Chisholm, M. H.; Extine, M. W. *J. Am. Chem. Soc.* **1977**, *99*, 792.
(12) Bellamy, L. J. "The Infrared Spectra of Complex Molecules"; Chapman and Hall: London, 1975.
(13) Adams, R. D.; Chodosh, D. F. *J. Am. Chem. Soc.* **1977**, *99* 6544.
(14) Adams, R. D.; Chodosh, D. F. *Inorg. Chem.* **1978**, *17*, 41.
(15) The low ν(CN) stretching frequency must be viewed with caution. Cf.: DeBoer, E. J. M.; Teuben, J. H. *J. Organomet. Chem.* **1979**, *166*, 193.

Contribution from Lash Miller Chemical Laboratories and Erindale College, University of Toronto, Toronto, Ontario, Canada

Selective, Naked Cluster Cryophotochemistry: Trisilver, Ag_3

Geoffrey A. Ozin,* Helmut Huber, and Steven A. Mitchell

Received March 1, 1978

A number of interesting observations have been made concerning the photoinduced diffusion/aggregation behavior of silver atoms isolated in cryogenic rare-gas supports.[1] The silver atomic diffusion process can be initiated and controlled by means of narrow-band UV photolysis centered at the atomic resonance absorption lines, and the aggregation processes can be followed by monitoring the optical spectra of the matrix deposits. These silver atom aggregation reactions provide a convenient and controlled route to matrix-isolated silver molecules, suitable for subsequent spectroscopic and cryochemical studies.[2] Similar photoaggregation processes have been reported for several other metal atomic species, including a number of the transition metals, in both uni- and bimetallic situations.[2,3]

A valuable insight into the mechanism of silver atom photomobilization has been obtained through fluorescence spectroscopic studies of matrix-isolated silver atoms.[4] Furthermore, it has become apparent from preliminary investigations that fluorescence studies have the potential for revealing a richly detailed picture of the photophysical behavior of matrix-isolated silver molecules. A combination of fluorescence spectroscopy and selective, narrow-band photolysis coupled with UV–visible spectral monitoring has now been used to explore the concept of silver cluster photochemistry. In this note we report UV–visible absorption results relating to trisilver visible photochemistry, a system which we believe to be somewhat unique in a number of respects. A more detailed account of the photophysical aspects of this work will appear in a subsequent publication.[4b] Selective Cu_2 and Ag_2 cryophotochemistry, emission spectroscopy, and SCF–Xα–SW molecular orbital calculations for Cu_2 and Ag_2 will also appear in a separate publication.[1c,4b]

The optical absorption bands attributed to Ag_{1-3} isolated in Ar, Kr, and Xe matrices[1,5] are illustrated in Figure 1. Because of the difficulties involved in arriving at an unambiguous correlation of absorption bands with specific cluster species, the assignments for some of the weaker features of the absorption spectra must be regarded as tentative. However, it is our contention that the results of the present study provide support for these assignments.

A detailed analysis of the trisilver absorption spectrum is subject to a number of complications. The Ag_3 band assignments, for example, must be based on a molecular orbital

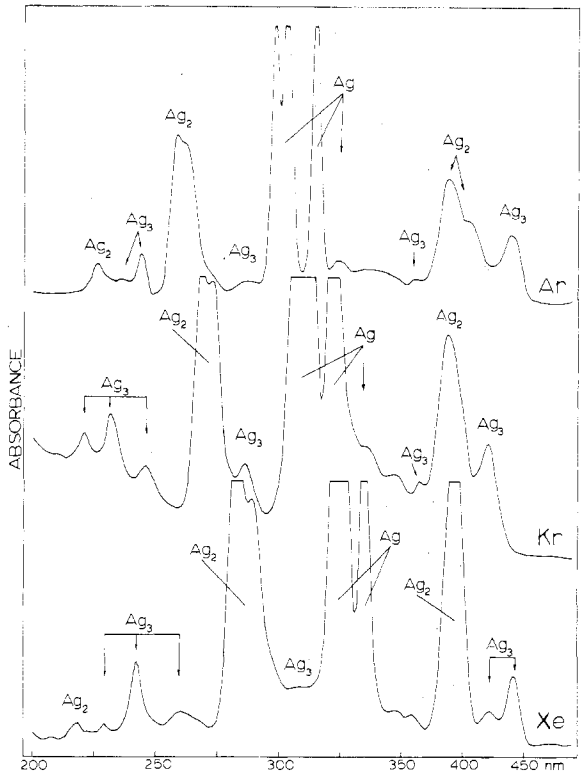

Figure 1. UV–visible spectra of Ag_{1-3}/(Ar, Kr, and Xe) mixtures generated by condensing silver atoms with the rare gases (Ag/matrix $\simeq 1/10^3$) at 12 K and irradiating the deposits at the frequencies of silver atomic resonance absorption lines.

model together with an assumed or predicted geometry,[6] since no gas-phase spectroscopic data are presently available for Ag_3. Additional complications arise from the possible coexistence of geometrical isomers or spectroscopically distinct matrix trapping sites.[7] In this connection, we believe that the photochemical studies described below show potential for elucidating the optical spectroscopic consequences of structural rearrangements of matrix-entrapped trisilver molecules.

The outcome of photoexcitation centered at the visible band of entrapped Ag_3 in Ag_{1-4}/Kr mixtures (Ag/Kr = $1/10^2$) at 12 K is illustrated in Figure 2. A comparison of spectrum B with spectrum A shows that major spectral changes result from the photolysis and that these alterations are restricted to the set of absorption bands believed to be associated with Ag_3. Thus, while the bands labeled Ag, Ag_2, and Ag_4 remain essentially invariant, each of the original Ag_3 bands undergoes a substantial decrease in intensity, and a number of new features appear, the most prominent of which is centered near 445 nm. Spectrum C in Figure 2 illustrates the interesting result that the effects of the visible trisilver photolysis can be essentially exactly reversed by a brief, 25 K thermal annealing period. Thus, the photoinduced transformation is thermally reversible and can be recycled many times without major modifications to the optical spectrum. Notable also is the observation that the original Ag_3 absorption spectrum can be similarly regenerated by irradiating the new band at 445 nm.

Figure 3 shows results for Xe matrices closely analogous to the Kr results illustrated in Figure 2, indicating a similar photochemical behavior of Xe- and Kr-entrapped trisilver. The results shown in Figures 2 and 3 indicate that visible Ag_3 photoexcitation in Kr and Xe matrices results in a highly selective, thermally and photolytically reversible trisilver phototransformation. These results for Kr and Xe supports are in distinct contrast to the results for Ar supports, where prolonged trisilver visible photoexcitation produces no observable changes in the optical spectrum. Recent fluorescence

0020-1669/79/1318-2932$01.00/0